Advances in Aircraft and Spacecraft Science, *Vol. 5, No. 3 (2018) 385-400*
DOI: https://doi.org/10.12989/aas.2018.5.3.385

Development of dynamic behavior of the novel composite T-joints: Numerical and experimental

Madjid Mokhtari*, Morteza Shahravi and Mahmood Zabihpoor

Department of Aerospace Engineering, Maleke-e-Ashtar University of Technology, Lavizan, Tehran, Iran

(Received September 10, 2017, Revised October 19, 2017, Accepted November 15, 2017)

Abstract. In this paper dynamic behavior (modal analysis and dynamic transient response) of a novel sandwich T-joint is numerically and experimentally investigated. An epoxy adhesive is selected for bonding purpose and making the step wise graded behavior of adhesive region. The effect of the step graded behavior of the adhesive zone on dynamic behavior of a sandwich T-joint is numerically studied. Finite element analysis (FEA) of the T-joints with carbon fiber reinforced polymer (CFRP) face-sheets is performed by ABAQUS 6.12-1 FEM code software. Modal analysis and dynamic half-sine transient response of the sandwich T-joint are presented in this paper. Two verification processes employed to verify the dynamic modeling of the manufactured sandwich panels and T-joint modeling. It has been shown that the step wise graded adhesive zone cases have changed the second natural frequency by about 5%. Also, it has been shown that the different arranges in the step wise graded adhesive zone significantly affect the maximum stresses due to transient dynamic loading by 1112% decrease in maximum peel stress and 691.9% decrease in maximum shear stress on the adhesive region.

Keywords: sandwich T-joints; step wise graded adhesive zone; transient dynamic loading; modal analysis

1. Introduction

Composite T-joints are finding wide range of applications in the aerospace, wind turbine, ship and automobile designs since these lightweight materials possess high specific strength and specific stiffness. Basically, to increase the load transfer of the joints efficiently, bonded/fastened joints are required for composite assemblies. More uniform stress distribution, better fatigue properties, removed stress concentration and reduced structural weight are the advantages of adhesively bonded composite joints in comparison with fastening techniques. Despite, stress concentration near the adhesive region ends forced researchers to improve the adhesive joints. Geometry improvements, better adhesive synthesis, surface treatments, and adhesive region with graded properties are the recent attempts to improve the capability of the adhesive joints to transfer much more load and minimize the edge effects and related stress concentration of the both side tip adhesive regions.

Sandwich panels with functionally graded (FG) face-sheets, FG cores and different thermal and boundary conditions were widely studied by authors in recent years by (Malekzadeh and

*Corresponding author, E-mail: m.mokhtari@mut.ac.ir

http://www.techno-press.org/?journal=aas&subpage=7 ISSN: 2287-528X (Print), 2287-5271 (Online)

Ghaedsharaf 2014), (Malekzadeh *et al*. 2015) and (Malekzadeh and Monajjemzadeh 2013).

Functionally graded adhesive joints (FGAJ) has been studied for the first time by Raphael (Raphael 1966). FG adherends studied by Apalak (Apalak *et al*. 2005) and (Apalak *et al*. 2014). They investigated three-dimensional elastic stress state of an adhesively bonded single lap joint with functionally graded adherends in tension. Their adherends were composed of a functionally gradient layer between a pure ceramic (Al_2O_3) layer and a pure metal (Ni) layer. They observed stress concentrations along the free edges of the adhesive layer and through the corresponding zones in the upper and lower adherends. They found that the layer number and compositional gradient exponent have an evident effect on the through-thickness profiles and magnitudes of the critical stress components in the adherends and adhesive layer of the functionally graded adhesively bonded joints.

Optimization of the FG adhesive joints based on the free vibration response of the single lap joint with FG adherends are investigated by Gunes *et al*. on (Gunes *et al*. 2007) and (Gunes *et al*. 2010). Three-dimensional free vibration and stress analysis of an adhesively bonded functionally graded single lap joint were carried out. The effects of the adhesive material properties, such as modulus of elasticity, Poisson's ratio and density were found to be negligible on the first ten natural frequencies and mode shapes of the adhesive joint. Finally, they have reported the optimal joint dimensions and compositional gradient exponent with the maximum natural frequency and the minimum modal strain energy as optimization target functions.

Tube FG adherends have been investigated to design an adhesive joint with the best dynamic response and increase on load transfer capability (Gunes *et al*. 2011, Kumar *et al*. 2013). Impact effect on FG adhesive joints by (Sun and Luo 2011, Bodaghi and Shakeri 2012, Kiani *et al*. 2013), FG coatings (Chidlow *et al*. 2013), FG adhesive patch repairing on civil structures (Carbas *et al*. 2015), failure criterion of FG adhesive joints (Miyamoto *et al*. 2013) and buckling of the FG structures (Uysal and Güven 2015) are the other attractive objects which are investigated by authors.

Implementation of the FG adhesive region is the main problem of the experimental researchers. Multi-adhesive region has been presented by Banea (Banea *et al*. 2017) to increase the performance of the aerospace adhesive joint under high temperature conditions. They used two adhesive types to attain the graded properties on adhesive region. The main problem in this method was the uncontrolled bounds of the adhesives and adhesive flowing during curing.

The next idea to FG implementation was the high temperature adhesive mixtures first reported by Hart-Smith (1973). Marques *et al*. (2013) have investigated the mixture effect of Resbond 940SS and Ceramabond 552 silica-based adhesives. Also, some authors studied the effect of adhesive mixtures like (Afkar *et al*. 2014), (da Silva and Adams 2007a, b). Undesired reactions between different resins and hardeners which are mixed and uncontrollable adhesive bounds are the main challenges of this FG region implementation. The strength and lifetime of the tubular joints have been studied by Kumar el al. They studied the effect of functionally graded bondlines on axisymmetric adhesive joints (Kumar 2009) (Kumar *et al*. 2013a, b).

Stapleton *et al*. numerically and analytically studied the effect of various boundary conditions and loading conditions of some typical adhesive joint geometry on selection of graded function in (Stapleton *et al*. 2012) and (Scott *et al*. 2017). The results of this study have been experimentally checked with graded dispersion of glass beads on adhesive region of a single lap adhesive joint.

Carbon black was the other material used by (Carbas *et al*. 2017) and (Andrés *et al*. 2015) subjected to implementation of the graded properties in adhesive region. This implementation was based on graded curing of the adhesive and various properties of special adhesives in various

curing temperatures. Dielectric properties of functionally distributed carbon black on adhesive region and UV curing of the adhesive region cause variable temperature curing on adhesive region. Adhesive flowing and perfect distribution of carbon black particles are the main uncertainty sources.

Variable curing temperature was the main attempt which cancelled the uncertainty problems of adhesive flowing and particle transformations. Carbas *et al*. experimentally checked induction heating process and post curing to attain graded properties on adhesive region in Carbas *et al*. (2014), Carbas *et al*. (2014) and Carbas *et al*. (2016). High energy consumption and both side accessibility are the main challenges of their proposed method. They have shown that the maximum load transfer capacity of the single lap joint with graded adhesive region was more than 40%.

After numerical investigation of single lap joints with composite adhesive region (Khalili and Mokhtari 2015), we are going to develop and study the effect of controlled variable adhesive region properties on titled FG adhesive zone.

In this paper dynamic behavior (modal analysis and dynamic transient response) of a novel sandwich T-joint is numerically and experimentally investigated. According to the literature Loctite Hysol 3422 properties, an epoxy adhesive is selected for bonding purpose and for making the step wise behavior of adhesive region based on variable curing temperatures. FEA of the T-joints with CFRP face-sheets, is performed by ABAQUS 6.12-1 FEM code software. Modal analysis and dynamic step transient response of the sandwich T-joint (according to our recent studies Khalili *et al*. 2014 and Mokhtari and Shahravy 2017) are presented in this paper. Step wise graded adhesive zone affect the second natural frequency by 5%. Also, it has been shown that the different arranges in the step wise graded adhesive zone significantly affect the maximum stresses due to transient dynamic loading by 1112% decrease in maximum peel stress and 691.9% decrease in maximum shear stress on the adhesive region.

2. Experimental details

Experimental works in this paper are concentrated on verification purposes to verify the 1-dynamic behavior of sandwich panel adherends and 2-T-joint dynamic response. All of the specimens are manufactured in the institute of Shahid Ghandi Center of Research (SGCR, Tehran, Iran). T-Joints are manufactured with E-glass/epoxy face-sheets and XPS high density core. CFRP sandwich panel was selected to verify the numerical dynamic analysis of the adherends. Due to two verification processes employed to verify the dynamic modeling of the T-joint, experimental details referred to manufacturing of the CFRP sandwich panel and T-joint manufacturing.

2.1 Manufacturing process of CFRP sandwich panels

T300 (Toray, USA) carbon fiber and Araldite 5052 (Huntsman, Chicago, USA) epoxy resin with 60% fiber fractions used for autoclave curing process ([45/0/45/0]) and AF-163 2K (3M, USA) adhesive film used for core bonding. Vacuum bag and pressure assisted process are chosen to manufacture the co-cured CFRP face-sheets and aluminium honeycomb core in autoclave. The manufacturing process of CFRP sandwich panel is shown in Fig. 1.

The sandwich panel specimens dimension was 320×250×16 mm and produced by high-precision milling of a larger plate. CFRP face-sheets were bonded to the Hexcel aluminium

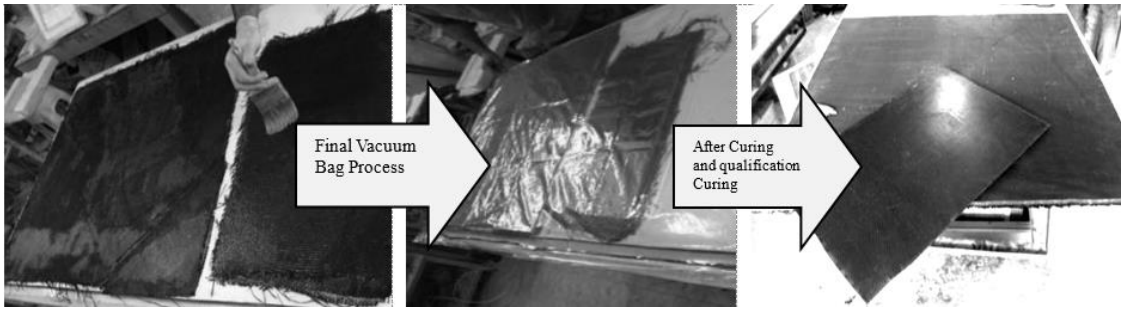

Fig. 1 Hand lay-up process, sandwich panel vacuum bag and pressure process and trimmed sandwich panel

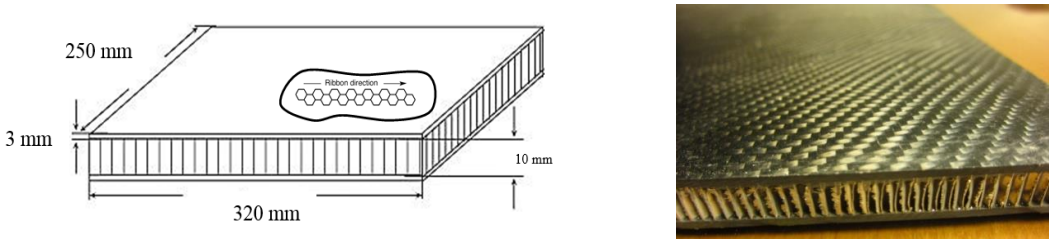

Fig. 2 Right: CFRP sandwich panel specimen used for modal test; Left: Geometry of CFRP sandwich panel specimen and ribbon direction

honeycomb core (HC-1/8-5052-.001) using AF-163 2K adhesive films. The specimen configurations and geometry are shown in Fig. 2.

2.2 Manufacturing process of the sandwich T-joint

T-joint specimens are manufactured with 3 layers of woven glass roving laminated with epoxy resin. The thickness of each layer is about 0.35 mm. These adherends were fabricated by hand lay-up stacking plies and cured in room temperature and compressed for 12 h at 25°C and 1.25 bar. The fiber volume fraction for the selected fabrication conditions (pressure, temperature and ply thickness) was 48%. The manufacturing process of the T-joint specimens are presented in Fig. 3.

2.3 Modal test

Modal test is the basic test to find the dynamic behavior of the structures. According to two selected verification processes for both of the adherend sandwich panels and the T-joints, separately the modal analysis of the sandwich panel of the adherends and T-joints were checked experimentally. A small adhesive thickness (about 0.35 mm) was used to ensure the strength of the face-sheet bonding. The adhesive thickness is controlled with some rigid particles like glass beads. Free-free boundary condition selected for modal analysis of all specimens. All free modal specimens were tested with the impact hammer test set-up shown in Fig. 4.

3. Numerical modeling

The numerical analysis of the joint was done using ABAQUS-6.12 (Dassault systems simulia,

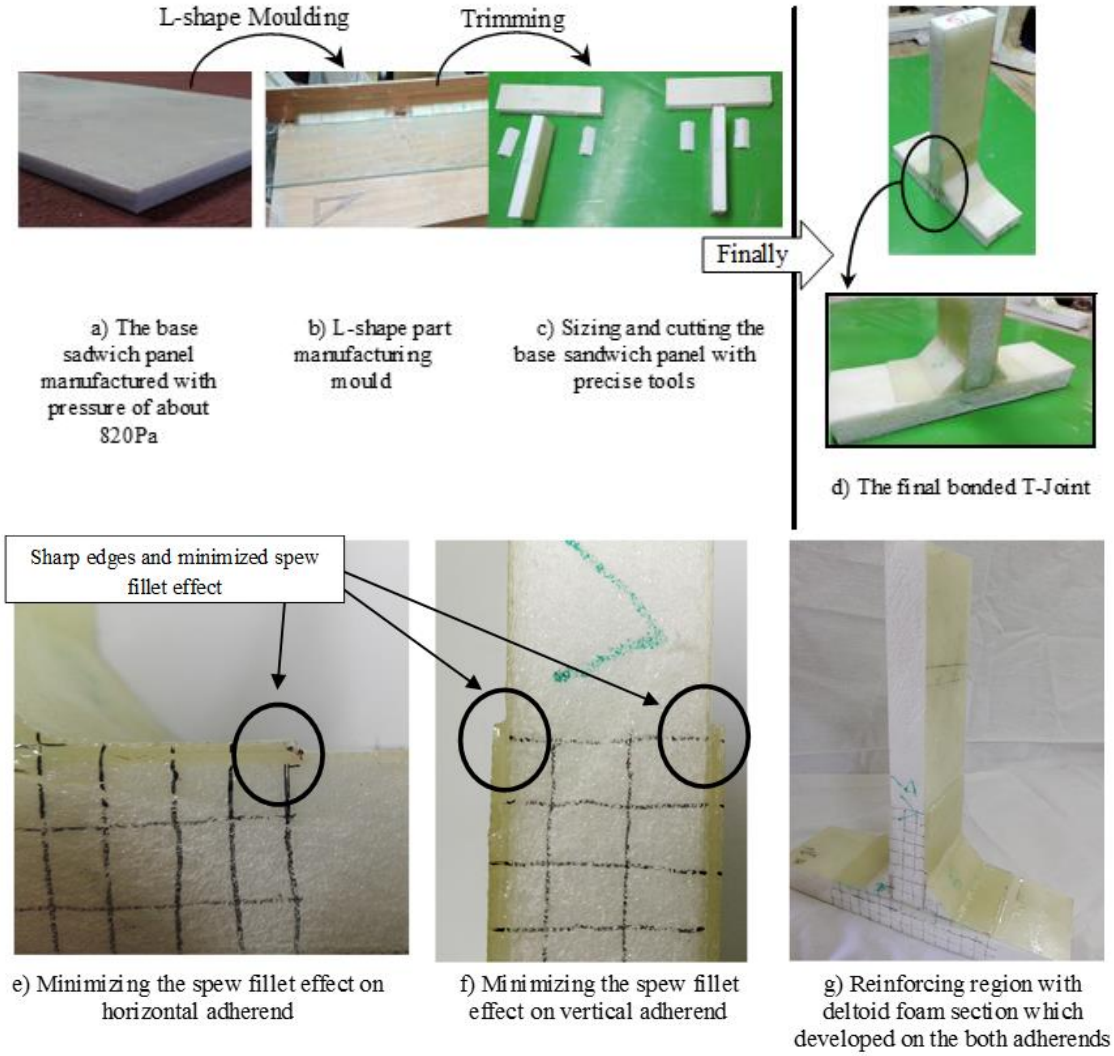

Fig. 3 Manufacturing process and details of the T-joint specimens for modal test

MA, USA) FE code. The behavior of all the members was assumed to be linear elastic. The above linear assumption was considered, since the adhesive used in the present work is quite brittle. The mesh study for the stabled magnitude of the first non-zero natural frequency was checked. The geometry of the sandwich panel and the sandwich panel T-joint used in this analysis are shown in Figs. 2 and 3. For verification purposes, the adherends, adhesive and geometry of the joint are considered similar to those used in the presented in presented experimental works. Transient dynamic loading condition and damage assessment of the T-joint adherends are modeled with CFRP face-sheets (mechanical properties are presented in Table 1) and T-joint modal specimen with glass/epoxy face-sheets (Mokhtari and Shahravi 2017) with mechanical properties of: E_{11}=22 GPa, E_{22}=18 GPa, G_{12}=30 GPa, υ_{12}=0.3, ρ=2200 kg/m^3 and XPS foam core (E_{11}=37.5 MPa, E_{22}=23.5 MPa, G_{12}=12.2 MPa, ρ=37.5 kg/m^3).

Numerical modeling of the sandwich panel done in two forms: 1- fully 2D geometry and

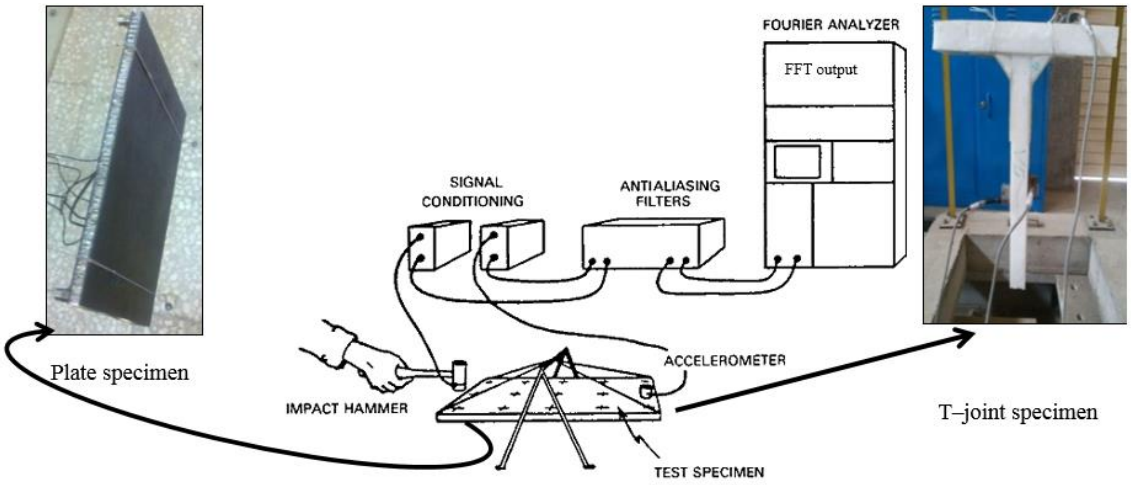

Fig. 4 Schematic of the modal test process for two series of specimens: T-joint specimen (right) and CFRP sandwich panel specimen (left)

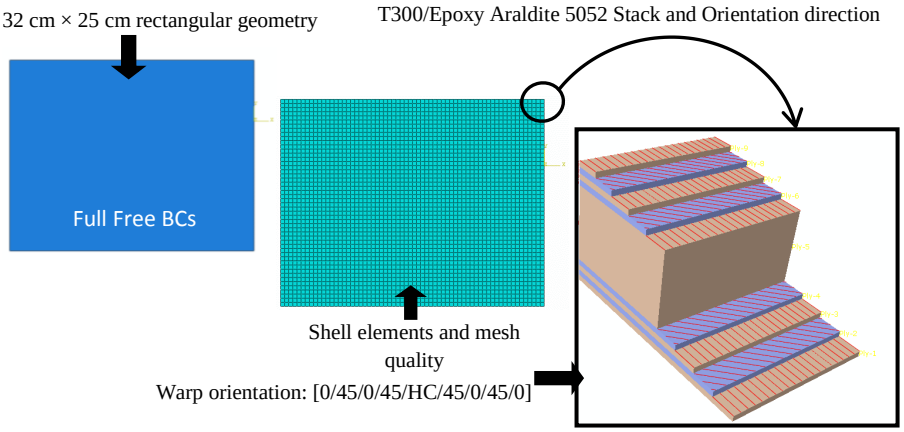

Fig. 5 Geometry, BCs, mesh size (3185 S4R ABAQUS linear shell elements) and composite lay-up of satellite sandwich panel FEM model (from left to right respectively)

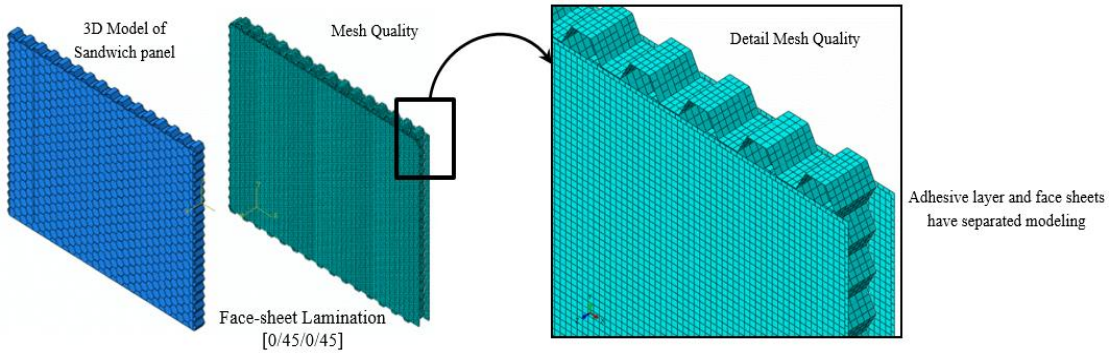

Fig. 6 Satellite sandwich panel with 3D core model: geometry, mesh size and detailed FE modeling of satellite sandwich panel FEM model (from left to right respectively)

SHELL (S8R) elements (Fig. 5) and 2-detailed modeling of the face-sheet, adhesive layer and honeycomb core with 2D elements (Fig. 6). Comparison of the modal results of the both numerical models are presented in Table 2.

Zero natural frequencies represent first six rigid body motions of free sandwich panel. Non-zero natural frequencies and mode shapes of FEM model and experimental results are compared to each other in Table 2.

As shown in Table 2, there is a maximum 10.76% discrepancy between the numerical and experimental results. According to Table 2, there is a good agreement between the mode shapes of numerical and experimental results of sandwich panel case.

SOLID (C3D8R) elements are used for meshing the T-joint adhesive joint (Figs. 7, 8). The width of all T-joints is 80 mm and the length of the both vertical and horizontal adherends are 230 mm. The thickness of the adherends was taken to be 25 mm (plain weaved glass/epoxy face-sheets [0/90/0] with 20 mm XPS foam core); with adhesive thickness of 0.4 mm.

Table 1 Mechanical properties of carbon/ epoxy (HTA 7/6376) (Olmedo 2012)

Longitudinal elastic modulus, E_1 (GPa)	145
Transverse elastic modulus, E_2 (GPa)	10.3
Transverse elastic modulus, E_3 (GPa)	11.1
In-plain shear modulus, G_{12} (GPa)	5.3
Out of plain shear modulus, G_{13} (GPa)	5.27
Out of plain shear modulus, G_{23} (GPa)	3.95
Main Poisson' ratio, υ_{12}	0.3
Through thickness Poisson' ratio, υ_{13}	0.5
Through thickness Poisson' ratio, υ_{23}	0.5
Longitudinal tensile strength (MPa)	2250
Longitudinal compression strength (MPa)	1600
Transverse tensile strength (MPa)	64
Transverse compression strength (MPa)	290
In plain shear strength, S_{12} (MPa)	120
In plain shear strength, S_{13} (MPa)	120
Out of plain shear strength, S_{23} (MPa)	50

Table 2 Comparison of experimental and numerical results of modal analysis of fully free boundary condition sandwich panel and T-joint specimens

	Mode #1	Mode #2	Mode #3	Mode #4	Mode #5
Experimental - Sandwich panel	545.16	846.10	1192.38	1227.39	1422.8
2D FEM Model - Sandwich panel	527.138	755.01	1155.9	1205.64	1424.39
2D detailed FEM Model - Sandwich panel	532.43	820.67	1160.56	1215.45	1424.6
% discrepancy (2D vs. Exp.) - Sandwich panel	3.30	10.76	3.05	1.77	0.11
First bending mode - Experimental - T-joint			778		
First bending mode - 3D FEM model - T-joint			895.046		
% discrepancy (3D vs. Exp.) - T-joint			15		

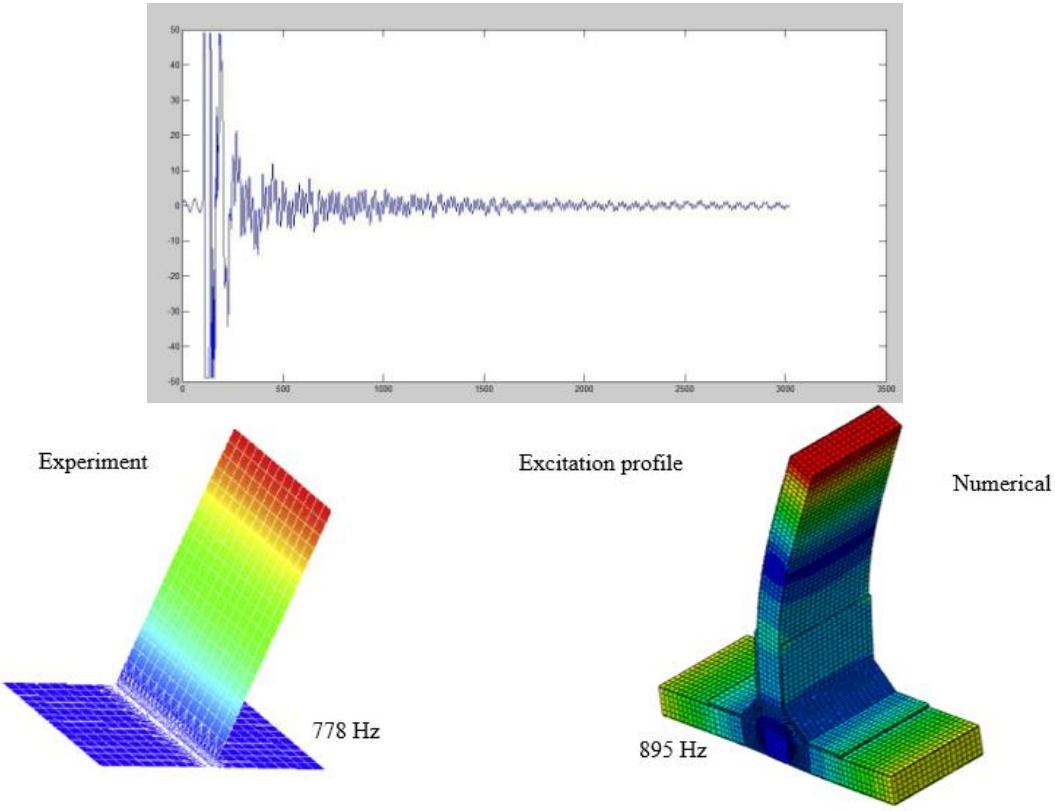

Fig. 7 Schematic mode shape of the first bending mode of the sandwich panel T-joint

Modal analysis results of a fully free boundary condition (Fig. 4) of T-joint sandwich panel was investigated after mesh study process and finding the best mesh size. Comparison of the first bending mode shape of numerical modeling and experimental results are shown in Table 2 and Fig. 7.

15% discrepancy between the first bending mode in numerical and experimental results of T - joint modal analysis is due to modal damping and specimen details like hyperelastic properties of the core which are neglected in FEM model.

3.1 Hashin's failure criterion

According to Hashin's criterion, four failure mechanisms are proposed to predict failures of composite structures. Hashin criterion In ABAQUS 6.12 FEM code for plain stress condition has presented the stress-strain relationship like Eq. (1)

$$\begin{Bmatrix}\sigma_1\\ \sigma_2\\ \tau_{12}\end{Bmatrix}=\begin{bmatrix}(1-d_f)E_1 & (1-d_f)(1-d_m)\nu_{21}E_1 & 0\\ (1-d_f)(1-d_m)\nu_{12}E_2 & (1-d_m)E_2 & 0\\ 0 & 0 & (1-d_s)GD\end{bmatrix}\begin{Bmatrix}\varepsilon_1\\ \varepsilon_2\\ \varepsilon_{12}\end{Bmatrix} \quad (1)$$

Where d_f belongs to fiber failure index, d_m belongs to matrix failure index and ds remark the shear failure. Mechanical properties of HTA 7/6376 carbon/epoxy composite are presented Table 1.

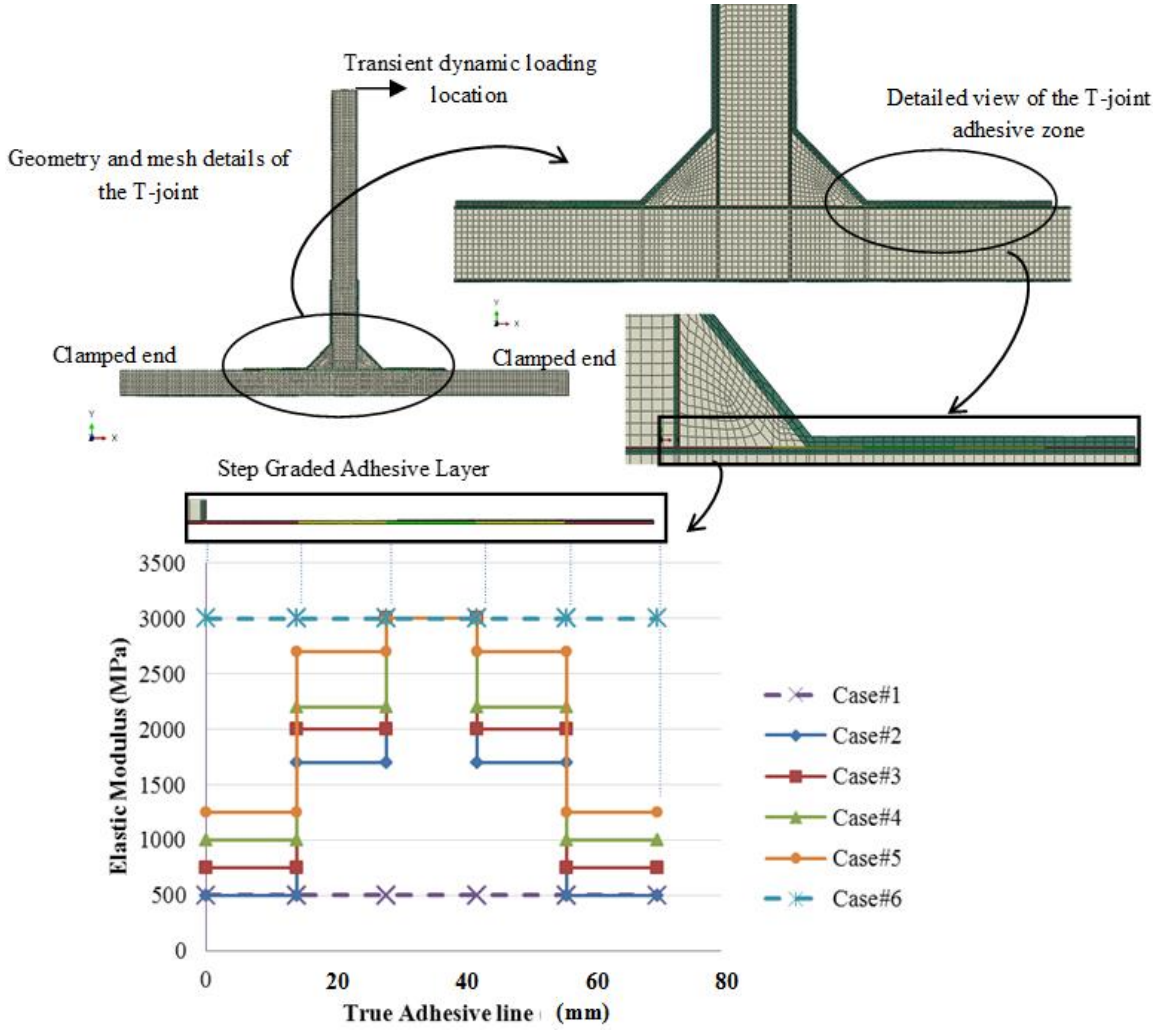

Fig. 8 Step graded adhesive zone details and 6 step wise graded reinforcing cases

Table 3 First five non-zero natural frequencies (Hz) of T-joint in the various arranges of the step graded adhesive layer cases in fully clamped horizontal adherend boundary conditions

	Mode #1	Mode #2	Mode #3	Mode #4	Mode #5
SGA - case 1	145.459	175.056	289.743	579.903	727.853
SGA - case 2	146.273	176.384	291.281	580.515	731.153
SGA - case 3	146.913	178.184	292.021	582.812	734.945
SGA - case 4	147.313	179.493	292.53	584.299	737.533
SGA - case 5	147.638	180.704	293.1	585.46	739.898
SGA - case 6	148.562	185.062	294.506	589.839	747.859
Comparison between cases # 1 & # 6 (%)	2.13	5.71	1.64	1.71	2.74
Comparison between SGAZ cases (%)	0.437	2.449	0.624	0.851	1.196
Comparison between SGAZ cases & case#1	0.999	3.226	1.158	0.958	1.654

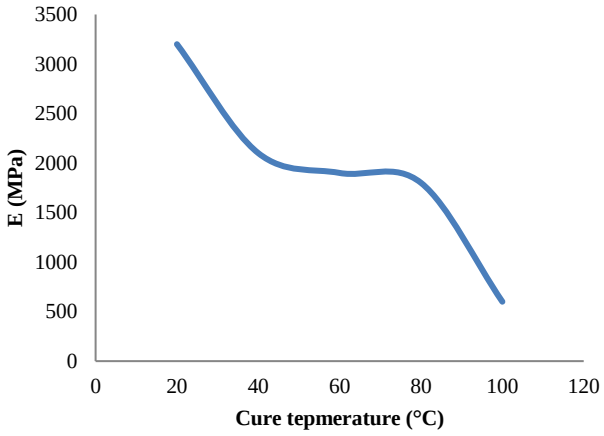

Fig. 9 Effect of curing temperature regimes on elasticity modulus of Hysol 3422 (Loctite Co.) epoxy adhesive (Carbas *et al*. 2014)

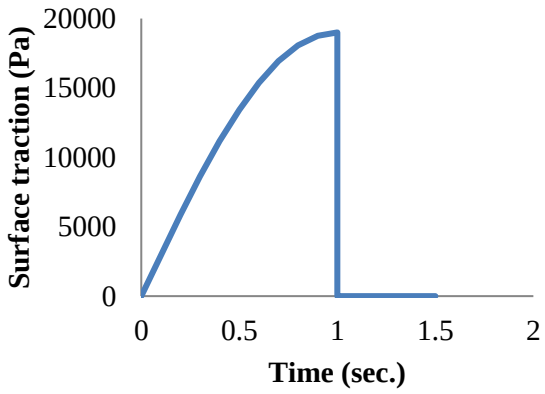

Fig. 10 Transient dynamic loading profile exerted to the Ver. Adherend tip to study the dynamic behavior of T-joint

Failure assessment was done to predict the probable failures of the T-joint adherends. Numerical analysis with consideration of progressive damage gives numerical results that are more consistent with experimental results, however progressive damage consideration increases the analysis costs.

3.2 Step wise graded adhesive zone (SGAZ)

Some mechanical properties like Young's modulus, yielding stress and toughness of some adhesives in different curing temperatures show significant differences. Most of papers have used FG adhesive materials as a virtual material with two ordinary margins also many of numerical and theoretical researchers found that the continuous change on adhesive bondline is the best choice to achieve the best load transfer capacity on adhesive joints. But the continuous and variable properties of adhesive bondline which obey a special function is not easy to perform. So, the 5

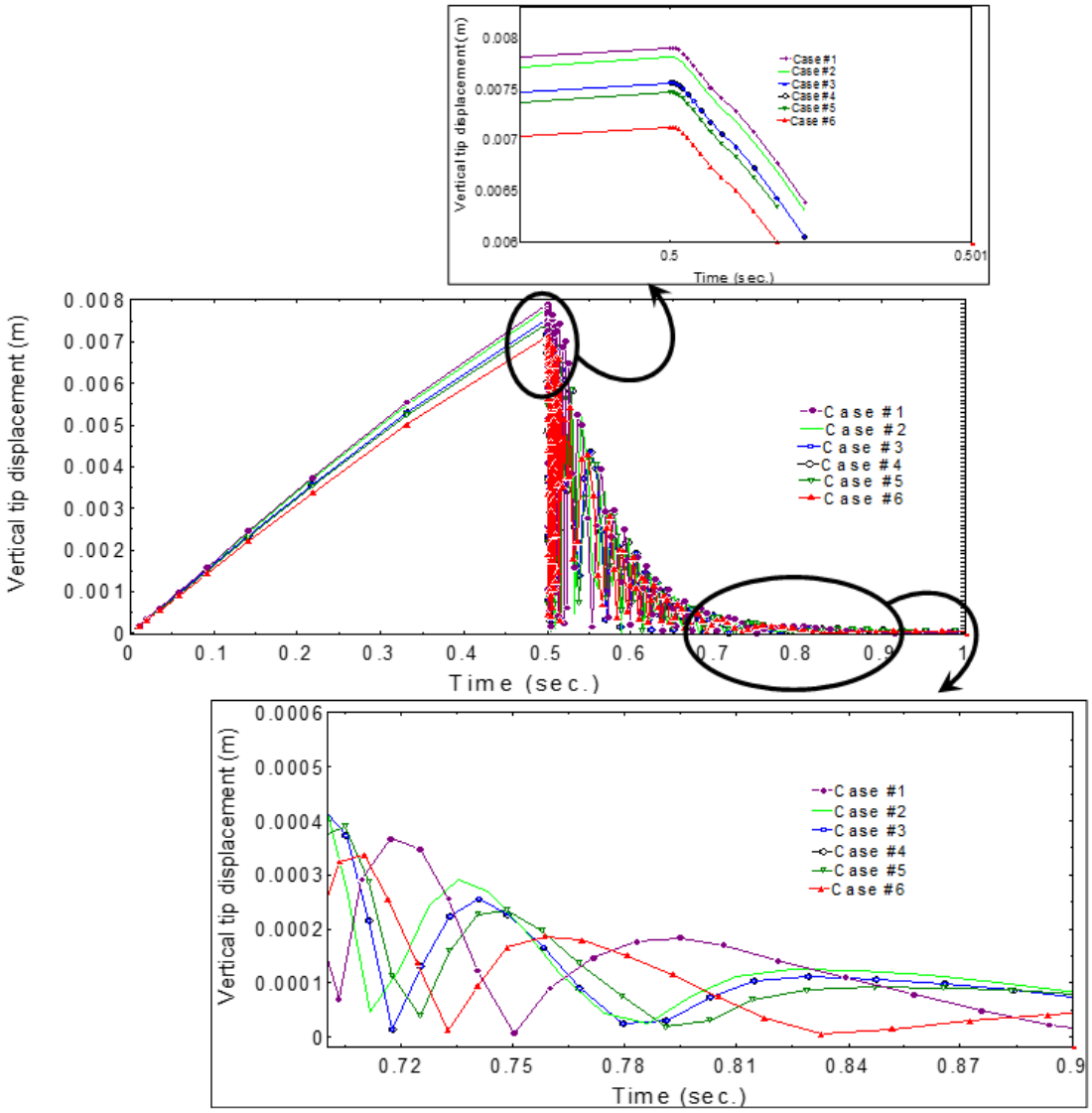

Fig. 11 Response of the vertical tip of T - joint during and after transient dynamic loading

applicable method is one which has the minimum adhesive region with accessible thicknesses; adhesive regions with 14 mm thickness chose to excess the load transfer capacity of the T-joint. The epoxy adhesive Hysol 3422 (Loctite Co.) is selected for numerical modeling due to excellent mechanical properties and different properties in different curing temperatures (Carbas 2013), (Fig. 9).

Graded adhesive region modeled in 6 cases is shown in Fig. 8.

The results of the first five non-zero natural frequencies of CFRP face-sheet T-joints in the various step graded adhesive layer cases in both side of the base adherend clamped boundary conditions (Fig. 8) are presented with separate comparison between 1-all cases, 2-SGAZ cases and SGAZ cases and 3-typical adhesive region (case # 1) in Table 3.

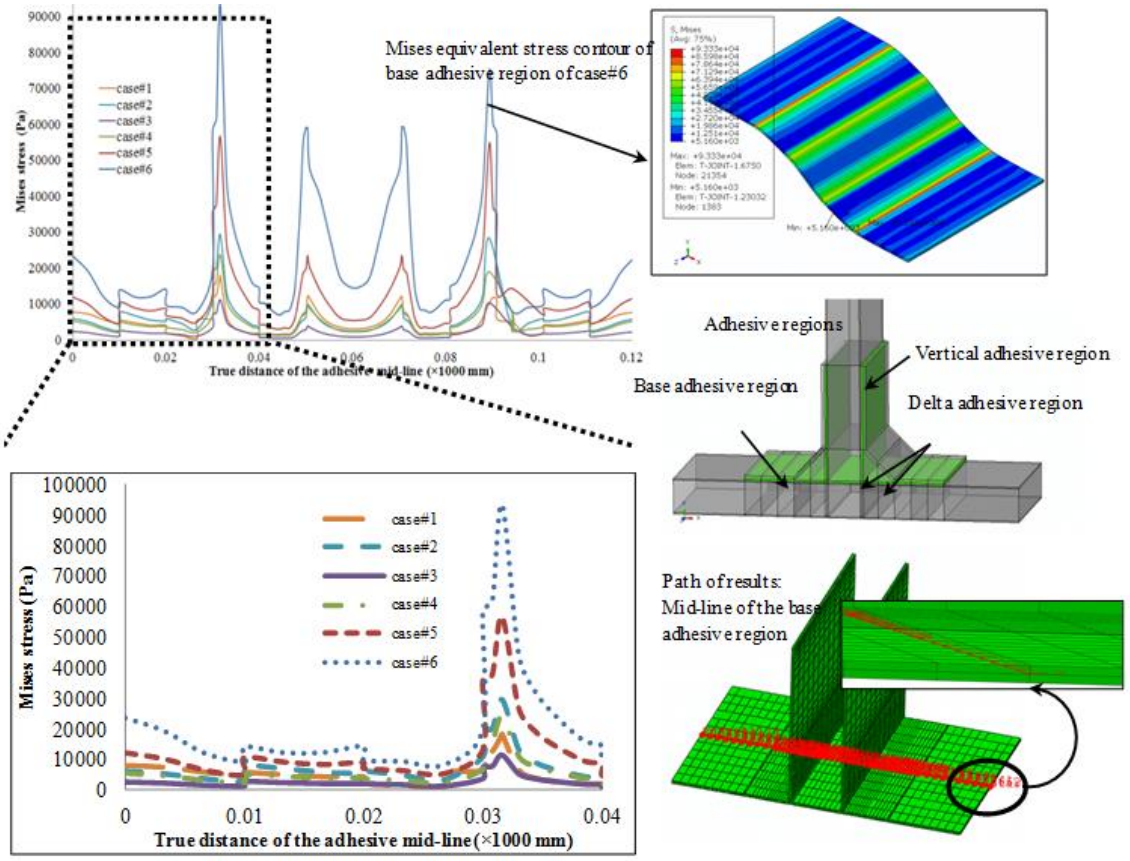

Fig. 12 Mises equivalent stress (Pa) results of mid-line path in the base adhesive region

3.3 Transient dynamic loading

The transient dynamic loading as step profile like Fig. 10 is exerted to the vertical adherend tip (Fig. 8) to study the dynamic behavior of T-joint. Dynamic response of the joint under transient dynamic loading, comparison of displacement domains and damping behavior of the joint, have been studied in this study. The response of this transient dynamic load, during 1 second after loading and subjected to the vertical tip of the T-joint, is given in Fig. 11. The schematic of loading direction is shown on Fig. 8. According to importance of adhesive layer, stress results are reported at the mid-line path of the base adhesive region. The equivalent Mises stress, peel stress and shear stress contours of six cases of step graded adhesive region are presented in Figs. 12-14, respectively. Sharp picks on Von Mises equivalent stress across a path line (Fig. 12) on the mid-line of adhesive region, is due to geometry and material changes and stress concentration of material changes are negligible in comparison with geometry changes. This behavior has been repeated for peel stress and shear stress which reported from the same path lines (Figs. 13-14).

Stress concentration due to edge effects on adhesive region near the edges is one of the major threads of adhesive joints; the effect of SGAZ cases on peel stress picks near the joint edge has been shown on Fig. 13.

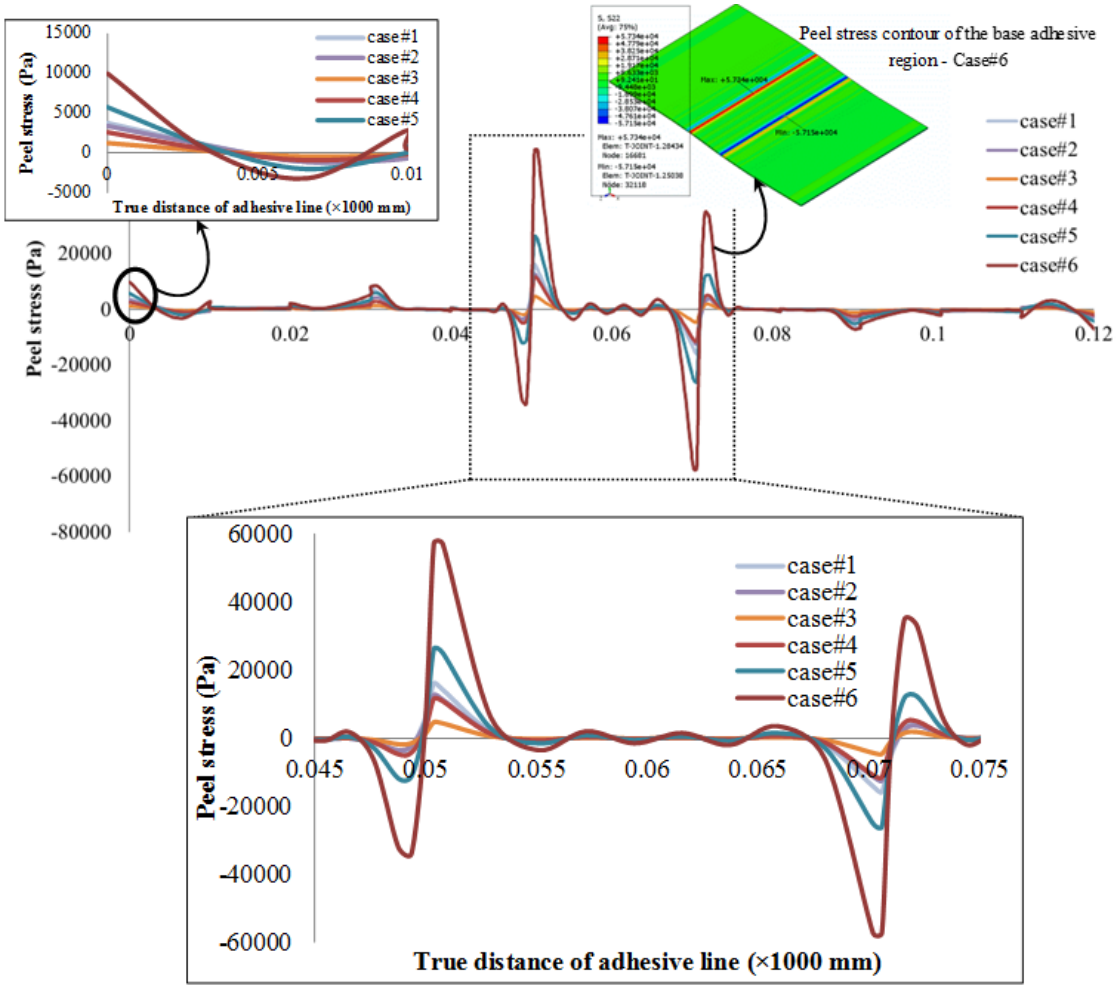

Fig. 13 Peel stress (S_{22}) (Pa) results of mid-line path in the base adhesive region

Table 1 Comparison of stress components (Pa) (Peel stress, shear stress and Mises) of the base adhesive region and effect of step graded adhesive region

	Case#1	Case#2	Case#3	Case#4	Case#5	Case#6	%discrepancy
Max. Peel Stress	16094.6	12730.9	4711.85	11575.2	26192.4	57150.4	1112.908
Max. Edge Peel Stress	3767.17	3394.1	1255.27	2603.29	5738.38	9972	694.4
Max. Shear Stress	6803.25	10926.1	4094.32	8554.7	19654.7	32426.6	691.9899
Max. Mises Stress	18126.1	29407.6	11222	23780.2	56624.7	93297	731.3759

To predict the failure mode of T-joint and study the effect of SGAZ cases Hashin's criteria chose. Results of Table 3 have been shown that the SGAZ case # 3 has the best reinforcing behavior among the other SGAZ cases. According to Hashin's criterion, failure index in cases # 3 and # 6 are presented at the worst failure index (Fig. 15) to predict the probable failure during and after the transient dynamic loading.

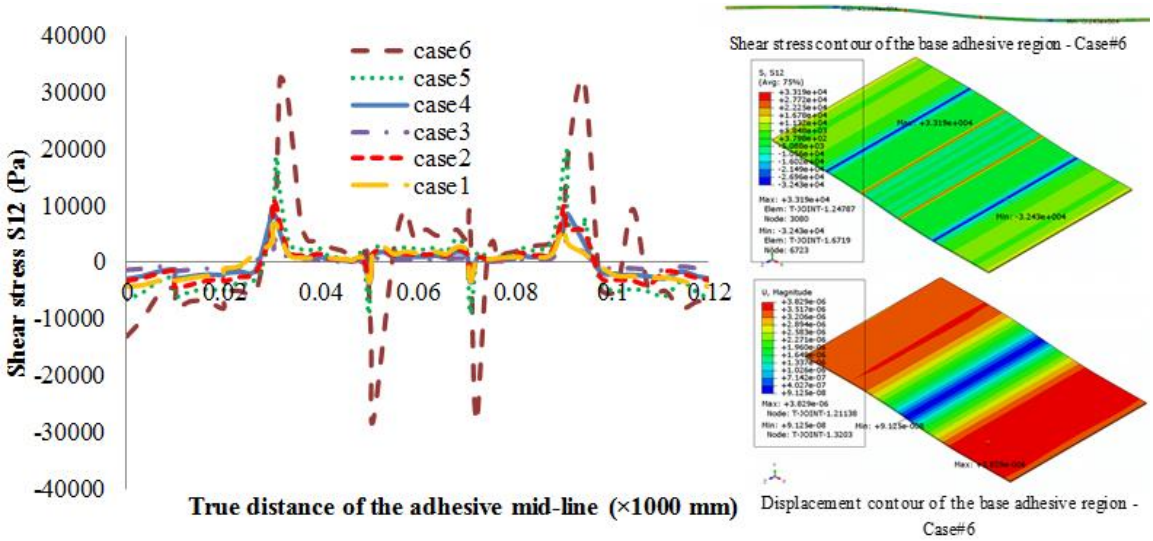

Fig. 14 Shear stress (S_{12}) (Pa) and displacement (m) contours and results of the mid-line path in the base adhesive region

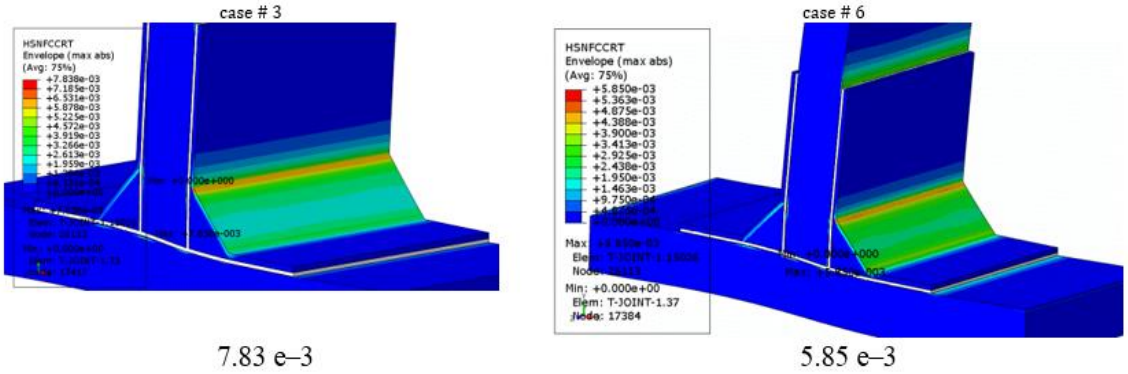

Fig. 1 Hashin's criterion failure index on the predicted failure mode

The effect of different SGAZ cases are reported respectively for the maximum stresses due to transient dynamic loading (peel stress pick, maximum shear stress and the maximum Mises equivalent stress) on the adhesive region (Table 4). Reported stress magnitudes are the results of a pure elastic model of adhesives and core materials and face-sheet composite materials with damage properties.

4. Conclusions

In this paper dynamic behavior (modal analysis and dynamic transient response) of a novel sandwich T-joint is numerically and experimentally investigated. FEA of the T-joints with CFRP face-sheets are performed by ABAQUS 6.12-1 FEM code software. Modal analysis and dynamic transient response of the sandwich T-joint are presented in this paper. Numerical result shown than the step wise graded adhesive zone case # 2 affect the second natural frequency by 3.1% more than

ordinary adhesive case # 1. Also, pure elastic modeling of the adhesive region shown that the different arranges in the step wise graded adhesive zone can affect the maximum stresses due to transient dynamic loading significantly, by decreasing the peel stress pick by 1112%, and the maximum shear stress by 691.9% and the maximum Mises equivalent stress on the adhesive region by 731.3% (Table 4). Comparison of peel stress and shear stress as main stresses describe the joint strength showed that the max. peel stress and shear stress, the T-joints with graded bondline (case #3) have shown a decrease 12.1 and 7.9 times lower than the homogeneous bondline respectively (stiff adhesive - case #6). Hashin's criterion was employed to predict the probable failure of T-joint with step graded improvement subjected to transient dynamic loading. Compression failure in fibers and fiber buckling is the predicted failure during transient dynamic loading. Although the minimum stresses are reported in case # 3, the compressive fiber failure index is more than case # 6 by 25%.

References

Afkar, A. and Camari, M.N. (2014), "Finite element analysis of mono-and bi-adhesively bonded functionally graded adherend", *J. Fail. Analy. Prev.*, **14**(2), 253-258.

Andrés, L.F.S., Carbas, R.J.C. and Da Silva, L.F.M. (2015), "Effect of carbon black nanoparticles concentration on the mechanical properties of an epoxy adhesive cured by dielectric heating", *Microsc. Microanal.*, **21**(S5), 15-16.

Apalak, Z.G., Ekici, R., Yildirim, M. and Apalak, M.K. (2014), "Free vibration analysis of an adhesively bonded functionally graded double containment cantilever joint", *J. Adhes. Sci. Technol.*, **28**(12), 1117-1139.

Banea, M.D., Da Silva, L.F.M., Carbas, R.J.C. and De Barros, D. (2017), "Debonding on command of multi-material adhesive joints", *J. Adhes.*, **93**(10), 756-770.

Bodaghi, M. and Shakeri, M. (2012), "An analytical approach for free vibration and transient response of functionally graded piezoelectric cylindrical panels subjected to impulsive loads", *Compos. Struct.*, **94**(5),1721-1735.

Carbas, R.J.C., Da Silva, L.F.M. and Andres, L.F.S. (2016), "Effect of carbon black nanoparticles concentration on the mechanical properties of a structural epoxy adhesive", *Proceedings of the Institution of Mechanical Engineers*, *Part L: Journal of Material*, *Design and Applications*, **232**(5), 403-415.

Carbas, R.J.C., Da Silva, L.F.M. and Andrés, L.F.S. (2017), "Functionally graded adhesive joints by graded mixing of nanoparticles", *Int. J. Adhes. Adhes.* **76**, 30-36.

Carbas, R.J.C., Da Silva, L.F.M. and Critchlow, G.W. (2014), "Adhesively bonded functionally graded joints by induction heating", *Int. J. Adhes. Adhes.*, **48**(5), 110-118.

Carbas, R.J.C., Da Silva, L.F.M. and Critchlow, G.W. (2014), "Effect of post-cure on adhesively bonded functionally graded joints by induction heating", *Proceedings of the Institution of Mechanical Engineers*, *Part L: Journal of Materials Design and Applications*, **229**(5), 419-430.

Carbas, R.J.C., Viana, G.M.S.O., Da Silva, L.F.M. and Critchlow, G.W. (2015), "Functionally graded adhesive patch repairs of wood beams in civil applications", *J. Compos. Construct.*, **19**(2).

Chidlow, S., Chong, W. and Teodorescu, M. (2013), "On the two-dimensional solution of both adhesive and non-adhesive contact problems involving functionally graded materials", *Eur. J. Mech. A-Solid.*, **39**, 86-103.

Da Silva, L.F.M. and Adams, R.D. (2007a), "Techniques to reduce the peel stresses in adhesive joints with composites", *Int. J. Adhes. Adhes.* **27**(3), 227-235.

Da Silva, L.F.M. and Adams, R.D. (2007b), "Adhesive joints at high and low temperatures using similar and dissimilar adherends and dual adhesives", *Int. J. Adhes. Adhes.*, **27**(3), 216-226.

Gunes, R., Apalak, M.K. and Yildirim, M. (2007), "The free vibration analysis and optimal design of an

adhesively bonded functionally graded single lap joint", *Int. J. Mech. Sci.*, **49**(4), 479-499.
Gunes, R., Apalak, M.K. and Yildirim, M. (2011), "Free vibration analysis of an adhesively bonded functionally graded tubular single lap joint", *J. Adhes.*, **87**(9), 902-925.
Gunes, R., Apalak, M.K., Yildirim, M. and Ozkes, I. (2010), "Free vibration analysis of adhesively bonded single lap joints with wide and narrow functionally graded plates", *Compos. Struct.*, **92**(1), 1-17.
Hart-Smith, L.J. (1973), *Adhesive Bonded Double-Lap Joints*, NASA-CR-112236, NASA.
Khalili, S.M.R. and Mokhtari, M. (2015), "Numerical study of adhesive single-lap joints with composite adherends subjected to combined tension-torsion loads", *J. Adhes.*, **91**(3), 214-234.
Khalili, S.M.R., Shariyat, M. and Mokhtari, M. (2014), "Static tensile and transient dynamic response of cracked aluminum plate repaired with composite patch-numerical study", *Appl. Compos. Mater.*, **21**(3), 441-455.
Kiani, Y., Sadighi, M., Salami, S.J. and Eslami, M. (2013), "Low velocity impact response of thick FGM beams with general boundary conditions in thermal field", *Compos. Struct.*, **104**, 293-303.
Kumar, S. (2009), "Analysis of tubular adhesive joints with a functionally modulus graded bondline subjected to axial loads", *Int. J. Adhes. Adhes.*, **29**, 785-795.
Kumar, S. and Scanlan, J.P. (2013), "On axisymmetric adhesive joints with graded interface stiffness", *Int. J. Adhes. Adhes.*, **41**, 57-72.
Kumar, S. and Scanlan, J.P. (2013a), "On axisymmetric adhesive joints with graded interface stiffness", *Int. J. Adhes. Adhes.*, **41**, 57-72.
Kumar, S. and Scanlan, J.P. (2013b), "Modeling of modulus graded axisymmetric adhesive joints", *J. Adhes.* **86**, 369-394.
Malekzadeh, K., Khalili, S.M.R. and Veysi Gorgabad, A. (2015), "Dynamic response of composite sandwich beams with arbitrary functionally graded cores subjected to low-velocity impact", *Mech. Adv. Mater. Struct.*, **22**(8), 605-618.
Malekzadeh, P. and Ghaedsharaf, M. (2014), "Three-dimensional free vibration of laminated cylindrical panels with functionally graded layers", *Compos. Struct.*, **108**, 894-904.
Malekzadeh, P. and Monajjemzadeh, S.M. (2013), "Dynamic response of functionally graded plates in thermal environment under moving load", *Compos. Part B: Eng.*, **45**(1), 1521-1533.
Marques, E.A.S. (2013), "Analysis of adhesive joints for aerospace applications", M.Sc. Dissertation, Porto University, Italy.
Miyamoto, Y., Kaysser, W.A., Rabin, B.H., Kawassaki, A. and Ford, G.R. (2013), *Functionally Graded Materials: Design*, *Processing and Applications*, Springer Science and Business Media, U.S.A.
Mokhtari, M. and Shahravy, M. (2017), "Numerical and experimental analysis of dynamical behavior of composite T-joint with step wise graded adhesive zone based on functional behavior model", *J. Sci. Technol. Compos.* **2**(2), 63-76.
Olmedo, Á. and Santiuste, C. (2012), "On the prediction of bolted single-lap composite joints", *Compos. Struct.*, **94**(6), 2110-2117.
Raphael, C. (1966), "Variable-adhesive bonded joints", *Proceedings of the Applied Polymer Symposium*, **3**, 99-108.
Stapleton, S.E., Waas, A.M. and Arnold, S.M. (2012), "Functionally graded adhesives for composite joints", *Int. J. Adhes. Adhes.*, **35**, 36-49.
Stapleton, S.E., Weimer, J. and Spengler, J. (2017), "Design of functionally graded joints using a polyurethane-based adhesive with varying amounts of acrylate", *Int. J. Adhes. Adhes.*, **76**, 38-46.
Sun, D. and Luo, S.N. (2011), "Wave propagation and transient response of a FGM plate under a point impact load based on higher-order shear deformation theory", *Compos. Struct.*, **93**(5), 1474-1484.
Uysal, M.U. and Güven, U. (2015), "Buckling of functional graded polymeric sandwich panel under different load cases", *Compos. Struct.*, **121**, 182-196.